Cao, X., Ni, B., Summers, D., Bortnik, J., Tao, X., Shprits, Y., Lou, Y., Gu, X., Fu, S., Shi, R., Xiang, Z., Wang, Q. (2017): Bounce resonance scattering of radiation belt electrons by H+ band EMIC waves. - *Journal of Geophysical Research*, *122*, 2, pp. 1702—1713.

DOI: http://doi.org/10.1002/2016JA023607

AGU PUBLICATIONS

JGR

Journal of Geophysical Research: Space Physics

RESEARCH ARTICLE
10.1002/2016JA023607

Key Points:
- EMIC waves can bounce-resonate with near-equatorially mirroring electrons
- Bounce resonance shows a strong dependence on L shell, wave normal angle distribution, and wave spectral properties
- Quantitative differences between bounce-resonant and cyclotron-resonant diffusion coefficients are presented

Correspondence to:
B. Ni,
bbni@whu.edu.cn

Citation:
Cao, X., et al. (2017), Bounce resonance scattering of radiation belt electrons by H^+ band EMIC waves, *J. Geophys. Res. Space Physics*, *122*, 1702–1713, doi:10.1002/2016JA023607.

Received 20 OCT 2016
Accepted 29 JAN 2017
Accepted article online 1 FEB 2017
Published online 10 FEB 2017

Bounce resonance scattering of radiation belt electrons by H^+ band EMIC waves

Xing Cao[1], Binbin Ni[1], Danny Summers[2], Jacob Bortnik[3], Xin Tao[4], Yuri Y. Shprits[5,6], Yuequn Lou[1], Xudong Gu[1], Song Fu[1], Run Shi[1], Zheng Xiang[1], and Qi Wang[1]

[1]Department of Space Physics, School of Electronic Information, Wuhan University, Wuhan, China, [2]Department of Mathematics and Statistics, Memorial University of Newfoundland, St. John's, Newfoundland, Canada, [3]Department of Atmospheric and Oceanic Sciences, University of California, Los Angeles, California, USA, [4]Department of Geophysics and Planetary Sciences, University of Science and Technology of China, Hefei, China, [5]Helmholtz Centre Potsdam, GFZ German Research Centre for Geosciences, Potsdam, Germany, [6]Department of Earth, Planetary, and Space Sciences, University of California, Los Angeles, California, USA

Abstract We perform a detailed analysis of bounce-resonant pitch angle scattering of radiation belt electrons due to electromagnetic ion cyclotron (EMIC) waves. It is found that EMIC waves can resonate with near-equatorially mirroring electrons over a wide range of L shells and energies. H^+ band EMIC waves efficiently scatter radiation belt electrons of energy >100 keV from near 90° pitch angles to lower pitch angles where the cyclotron resonance mechanism can take over to further diffuse electrons into the loss cone. Bounce-resonant electron pitch angle scattering rates show a strong dependence on L shell, wave normal angle distribution, and wave spectral properties. We find distinct quantitative differences between EMIC wave-induced bounce-resonant and cyclotron-resonant diffusion coefficients. Cyclotron-resonant electron scattering by EMIC waves has been well studied and found to be a potentially crucial electron scattering mechanism. The new investigation here demonstrates that bounce-resonant electron scattering may also be very important. We conclude that bounce resonance scattering by EMIC waves should be incorporated into future modeling efforts of radiation belt electron dynamics.

1. Introduction

Charged particles trapped by the Earth's magnetic field undergo three types of periodic motion: cyclotron, bounce, and drift. Each periodic motion can be associated with an adiabatic invariant. Resonant interactions between plasma waves and particles can violate the invariants and result in irreversible changes to the particle dynamics, cumulatively leading to variations of the particle phase space density. Many studies have demonstrated that cyclotron-resonant interactions with waves play an essential role in the scattering loss and acceleration of radiation belt electrons [e.g., *Horne and Thorne*, 1998; *Summers et al*., 1998, 2007a, 2007b; *Shprits et al*., 2008a; *Thorne*, 2010] and that drift resonant interactions significantly contribute to electron radial diffusion [e.g., *Elkington et al*., 2003; *Shprits et al*., 2008b; *Hudson et al*., 2014]. Bounce-resonant wave-particle interactions, however, have received much less attention so far.

It was *Roberts and Schulz* [1968] who suggested that bounce resonance with hydrodynamic waves could act as a feeding mechanism for electron pitch angle scattering by whistler mode waves. *Shprits* [2009] further proposed that both magnetosonic waves and electromagnetic ion cyclotron (EMIC) waves have the potential to resonate with near-equatorially mirroring electrons over a wide range of energies. Following the early work of *Roberts and Schulz* [1968], a recent study by *Li et al*. [2015] derived the formalism of bounce-resonant diffusion coefficients for spatially confined magnetosonic waves and quantitatively showed that bounce-resonant diffusion coefficients can be comparable to the gyroresonant diffusion coefficients for magnetosonic waves. A subsequent study by *Shprits* [2016] presented calculations of the bounce-resonant scattering of near-equatorially mirroring electrons by magnetosonic waves and explored the sensitivity of bounce-resonant diffusion coefficients to the resonance harmonic and assumed wave normal angle. Nonlinear processes of bounce resonance due to magnetosonic waves were proposed by *Chen et al*. [2015] and *Maldonado et al*. [2016] to interpret the transport of 90° pitch angle electrons to lower pitch angles.

While EMIC wave-driven electron cyclotron resonance has been comprehensively analyzed, to the best of our knowledge, there is currently no study aimed at understanding the bounce-resonant electron interactions with EMIC waves. Therefore, the present study is focused on the investigation of the bounce-resonant

interactions between EMIC waves and radiation belt electrons and the quantification of the corresponding rates of electron pitch angle scattering. We will clearly demonstrate that the bounce resonance scattering of radiation belt electrons by EMIC waves is critically important to radiation belt energetic electron dynamics, in particular for the electron population near 90° equatorial pitch angles.

2. Model of Bounce-Resonant Diffusion

To quantitatively investigate the role of EMIC waves in bounce-resonant electron scattering of electrons, we calculate the bounce-resonant pitch angle diffusion coefficients $D_{\alpha\alpha}$, using the method of *Tao and Li* [2016], which is extended from *Roberts and Schulz* [1968] and *Li et al.* [2015], to consider an arbitrary wave normal angle distribution for a given wave frequency. The equations to compute $D_{\alpha\alpha}$ are given as

$$D_{\alpha\alpha} = D_{\mathrm{WW}}\left(\frac{\sin^2(\alpha_{\mathrm{eq}})\tan\alpha_{\mathrm{eq}}}{2MB_{\mathrm{eq}}}\right)^2 \text{ and} \tag{1}$$

$$D_{\mathrm{WW}} = \frac{1}{2\pi}\left(\frac{p\cos\alpha_{\mathrm{eq}}}{m_e}\right)^2 \sum_{l=1}^{\infty}\int \mathscr{F}(\omega, k_{\parallel})\left[(\Delta W_{1l} + \Delta W_{2l})^2 + (\Delta W_{3l})^2\right] dk_{\parallel}, \tag{2}$$

where

$$\mathscr{F}(\omega, k_{\parallel}) = q^2\mathscr{E}_{\parallel}(\omega, k_{\parallel}) + \frac{M^2}{\gamma^2}k_{\parallel}{}^2\mathscr{B}_{\parallel}(\omega, k_{\parallel}), \tag{3}$$

$$\Delta W_{1l} = \frac{l}{z_i}J_l(z_i)[2\theta_m + \sin(2\theta_m)], \tag{4}$$

$$\Delta W_{2l} = \sum_{\substack{|l'-l|\neq 1 \\ l'-l=\mathrm{odd}}} J_{l'}(z_i)\left[\frac{\sin(l_+\theta_m)}{l_+} + \frac{\sin(l_-\theta_m)}{l_-}\right], \tag{5}$$

$$\Delta W_{3l} = \sum_{l'-l=\mathrm{even}} J_{l'}(z_i)\left[\frac{\cos(l_+\theta_m) - 1}{l_+} + \frac{\cos(l_-\theta_m) - 1}{l_-}\right]. \tag{6}$$

Here α_{eq} is the particle equatorial pitch angle, $M = \frac{p^2\sin^2\alpha_{\mathrm{eq}}}{2m_eB_{\mathrm{eq}}}$ is the first adiabatic invariant, B_{eq} is the geomagnetic field intensity at the Earth's equator, m_e is the electron rest mass, p is the electron momentum, ω denotes the wave frequency, $k_{\parallel}$ denotes the parallel component of wave normal, q denotes the particle charge, γ is the Lorentz factor, $\mathscr{F}(\omega, k_{\parallel})$ is the power spectral density of wave-induced external fluctuating force acting on an oscillating particle, and $\mathscr{E}_{\parallel}$ and $\mathscr{B}_{\parallel}$ are the parallel components of the power spectral densities of wave electric and magnetic fields, respectively. J is the Bessel function of the first kind, with argument $z_i = v_{\parallel}k_{\parallel}/\omega_b$, l is the resonance harmonic, and $l_{\pm} = l' - l \pm 1$. θ_m is given by the following equation:

$$\theta_m = \begin{cases} \arcsin(s_m/s_0), & s_m < s_0 \\ \pi/2, & s_m \geq s_0 \end{cases}, \tag{7}$$

where $s_0 = p\cos\alpha_{\mathrm{eq}}/(\gamma m\omega_b)$ and s_{m} denotes the distance from the equator to the boundary of EMIC waves along the field line and can be easily obtained from $s_{\mathrm{m}} = \frac{1}{2}[\sin\lambda_m\sqrt{3\sin^2\lambda_m + 1} + \ln\left(\sqrt{3\sin^2\lambda_m + 1} + \sqrt{3}\sin\lambda_m\right)/\sqrt{3}]LR_E$ for the adopted dipole geomagnetic field model. λ_m is the maximum latitude of EMIC wave coverage along the field line, R_E is the Earth's radius, and ω_b is the particle bounce frequency, given by [*Lenchek et al.*, 1961; *Roederer*, 1970; *Schulz and Lanzerotti*, 1974]

$$\omega_b = 2\pi\beta c/\left(4LR_ET(\alpha_{\mathrm{eq}})\right), \tag{8}$$

where $\beta = v/c$, v is the velocity of particle, c is the velocity of light, and $T(\alpha_{\mathrm{eq}}) = 1.3802 - 0.31987\left(\sin(\alpha_{\mathrm{eq}}) + \sqrt{\sin(\alpha_{\mathrm{eq}})}\right)$. The bounce resonance condition is as follows [*Shprits*, 2009; *Chen et al.*, 2015; *Li et al.*, 2015]:

$$\omega = l\omega_b. \tag{9}$$

In the present study, the EMIC wave spectral density is assumed to be Gaussian, given by [e.g., *Lyons*, 1974; *Glauert and Horne*, 2005; *Summers et al*., 2007b; *Ni et al*., 2015; *Shprits*, 2016]

$$\mathscr{B}(\omega) = A\exp\left[-\left(\frac{\omega-\omega_m}{\delta\omega}\right)^2\right] \quad (\omega_{lc}\leq\omega\leq\omega_{uc}), \tag{10}$$

where

$$A = \frac{B_w^2}{\delta\omega}\frac{2}{\pi^{1/2}}\left[\mathrm{erf}\left(\frac{\omega_m-\omega_{lc}}{\delta\omega}\right)+\mathrm{erf}\left(\frac{\omega_{uc}-\omega_m}{\delta\omega}\right)\right]^{-1}. \tag{11}$$

Here ω_{lc} and ω_{uc} are the lower and upper frequency limits of the wave spectrum, ω_m is the frequency with peak wave power, and $\delta\omega$ is the wave spectral bandwidth. Meanwhile, the wave normal angle distribution is also assumed to be Gaussian, given by [*Glauert and Horne*, 2005; *Albert*, 2007; *Ni et al*., 2015; *Cao et al*., 2016; *Tao and Li*, 2016]

$$g(\phi) = \exp\left[-\left(\frac{\tan\phi-\tan\phi_m}{\tan\phi_w}\right)^2\right] \quad (\phi_{lc}\leq\phi\leq\phi_{uc}), \tag{12}$$

where ϕ is the wave normal angle, ϕ_w is the angular width, ϕ_m is the normal angle with peak wave power, and ϕ_{lc} and ϕ_{uc} are the lower and upper bounds to the wave normal angle distribution. Then we obtain the wave number k from the general dispersion relation of electromagnetic waves in a cold magnetized plasma [*Stix*, 1962], given by

$$D(\omega,k,\phi) = \left(S\tan^2\phi+P\right)\mu^4-\left(RL\tan^2\phi+PS\left(2+\tan^2\phi\right)\right)\mu^2+PRL\left(1+\tan^2\phi\right)=0, \tag{13}$$

where $\mu=|k|c/\omega$ is the wave refractive index and R, L, S, and P are the Stix parameters given by

$$S=\frac{1}{2}(R+L), \quad D=\frac{1}{2}(R-L), \tag{14}$$

$$R = 1-\sum_s\frac{\omega_{ps}^2}{\omega(\omega+\omega_s)}, \tag{15}$$

$$L = 1-\sum_s\frac{\omega_{ps}^2}{\omega(\omega-\omega_s)}, \text{and} \tag{16}$$

$$P = 1-\sum_s\frac{\omega_{ps}^2}{\omega^2}, \tag{17}$$

in which $\omega_{ps}=(N_s{q_s}^2/m_s\varepsilon_0)^{1/2}$ are plasma frequencies and $\omega_s=q_sB/m_s$ are cyclotron frequencies of four particle species $s=e$, p, He^+, and O^+. N_s is the number density of particle species s, ε_0 is the vacuum dielectric constant, q_s is the particle charge, B is the geomagnetic field strength, and m_s is the particle rest mass.

3. Numerical Results

Figure 1 shows the line plots of proton and helium gyrofrequencies and the first to fifth harmonics of electron bounce frequency as a function of L shell for the indicated three electron kinetic energies (from left to right: 0.1, 1, and 10 MeV). The dipole magnetic field is adopted to calculate the ion gyrofrequencies. Due to the weak dependence of bounce frequency on the equatorial pitch angle (e.g., equation (8)), we consider the bounce frequency of $\alpha_{eq}=90°$ electrons in this figure. It is clearly shown that contributions from the resonance orders $l=1$ to 5 have the potential for bounce-resonant scattering of >100 keV radiation belt electrons. Since an increase of electron energy will increase the corresponding bounce frequency, only the first three harmonics contribute to the pitch angle diffusion of relativistic (>1 MeV) electrons in the outer radiation belt. While H^+ band EMIC waves can potentially drive bounce resonance with electrons over a broad energy range from 0.1 MeV to 10 MeV, He^+ band waves, with frequencies below the helium gyrofrequency, can only resonate with electrons with energies less than hundreds of keV at low L shells. Bounce resonance by H^+ band EMIC waves can occur over a much broader range of both L shell and electron energies. Therefore, this study focuses on investigating the role of H^+ band EMIC waves in driving the bounce-resonant scattering of outer radiation belt electrons.

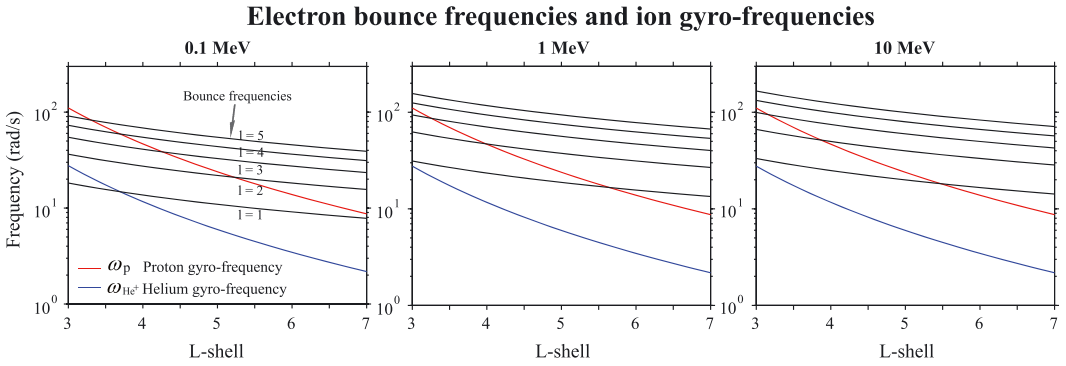

Figure 1. Ion gyrofrequencies and harmonics of electron bounce frequencies as a function of L shell for the indicated three electron kinetic energies (from left to right: 0.1, 1, and 10 MeV).

Figure 2 displays the electron bounce-resonance regions in the (E_k, L shell) space for $\alpha_{eq} = 90°$ electrons by EMIC waves corresponding to resonance harmonics $l = 1–3$. The dashed lines indicate the proton and helium ions gyrofrequencies, and the grey regions denote the resonance regions for a typical H^+ band frequency spectrum adopted from previous studies [e.g., *Summers and Thorne*, 2003; *Summers et al.*, 2007a], that is, $\omega_{lc} = 0.5\omega_p$, $\omega_{uc} = 0.7\omega_p$, $\omega_w = 0.1\omega_p$, and $\omega_m = 0.6\omega_p$. Given the resonance order, the electron bounce-resonance region due to H^+ band EMIC waves is strictly determined by the wave spectral lower and upper bounds, illustrating that a wider wave frequency spectrum results in a broader bounce-resonance region. As the resonance order increases, the electron bounce-resonance shifts to lower energies and lower L shells. Owing to the spectral upper limit at the proton gyrofrequency, EMIC waves cannot undergo bounce resonance with relativistic (>1 MeV) electrons for L > ~6.

In this study, we adopt a relatively strong wave amplitude B_w of 1 nT based on the statistical observations of H^+ band EMIC waves [e.g., *Min et al.*, 2012; *Meredith et al.*, 2014]. The results for arbitrary wave amplitude can be easily obtained, since diffusion coefficients are proportional to the square of wave amplitude in the quasi-linear regime (e.g., equation (11)). We adopt the dipole geomagnetic field model and set the maximum latitudinal coverage of EMIC waves $\lambda_m = 40°$, following the studies of *Ni et al.* [2015] and *Cao et al.* [2016]. We set the ion concentration ratios as $\eta_1 = 0.85$, $\eta_2 = 0.1$, and $\eta_3 = 0.05$ for hydrogen (H^+), helium (He^+), and oxygen (O^+), respectively [*Albert*, 2003; *Meredith et al.*, 2003; *Summers et al.*, 2007a; *He et al.*, 2016], where $\eta_1 = N_p/N_e$, $\eta_2 = N_{He^+}/N_e$, and $\eta_3 = N_{O^+}/N_e$. In addition, we take a quasi-parallel propagation model for the wave normal angle distribution by adopting $\phi_{lc} = 0°$, $\phi_{uc} = 20°$, $\phi_m = 10°$, and $\phi_w = 10°$ in equation (12) as a reference model.

In order to investigate the sensitivity of electron bounce-resonant pitch angle diffusion coefficients by H^+ band EMIC waves to the variations of L shell and electron number density, we choose three L shells (L = 3–5) and three specific electron densities, $N_e = 10^2$, 5×10^2, and 10^3 cm^{-3}, characteristic of the plasmasphere

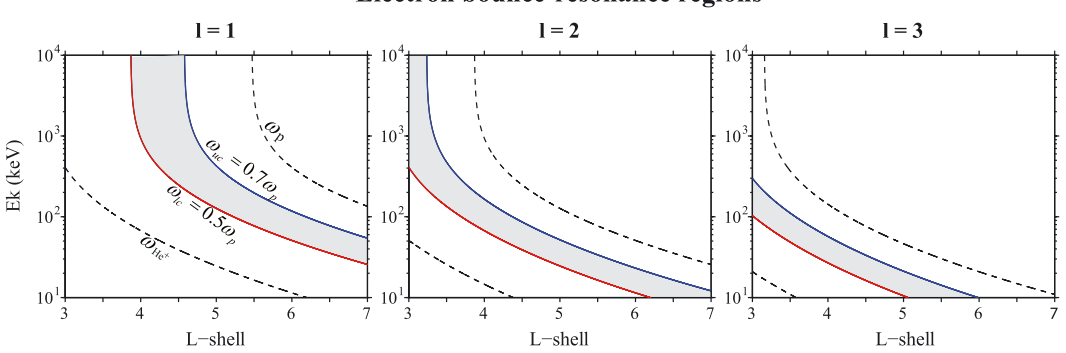

Figure 2. Electron bounce-resonance regions as a function of L shell and electron kinetic energy E_k for different resonance harmonics ($l = 1–3$) with H^+ band EMIC waves. The dashed lines denote the proton and helium gyrofrequencies in the dipole field, and the red and blue lines denote the lower and upper frequency limits of adopted H^+ band EMIC wave spectrum, respectively.

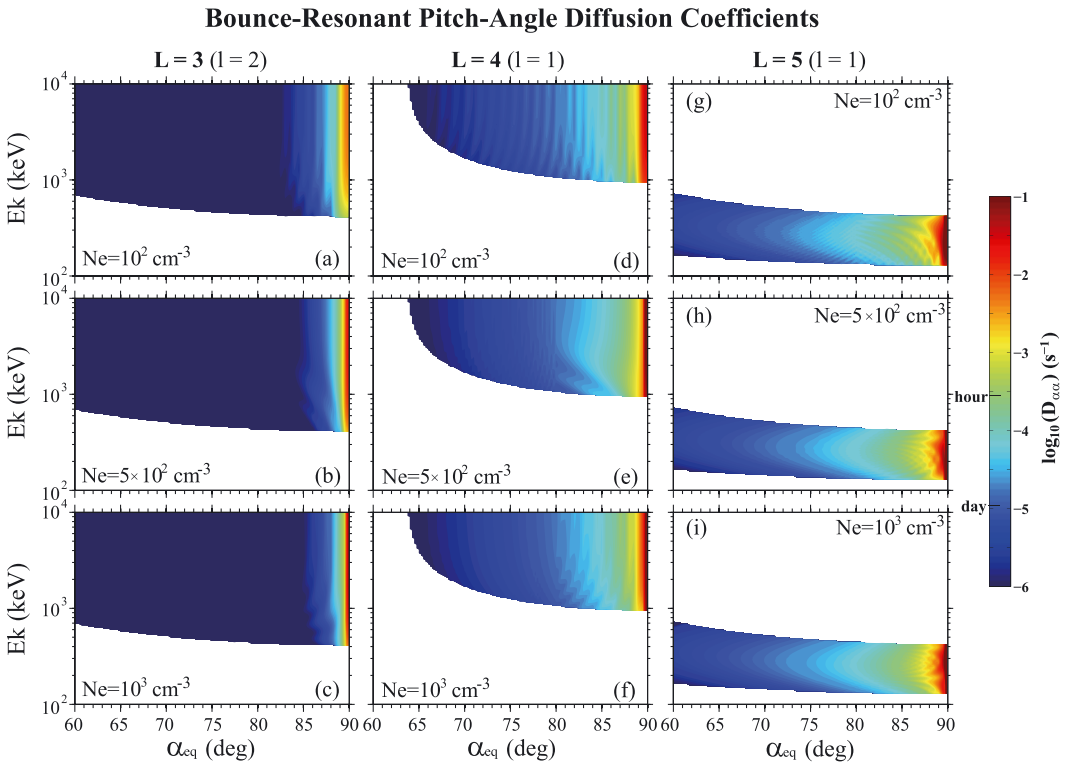

Figure 3. 2-D plot of bounce-resonant pitch angle diffusion coefficients due to H^+ band EMIC waves as a function of electron kinetic energy E_k and equatorial pitch angle α_{eq} for the indicated sets of L shell, bounce resonance harmonic l, and electron number density N_e. The wave amplitude B_w is 1 nT; the wave frequency spectrum is Gaussian with $\omega_{lc} = 0.5\omega_p$, $\omega_{uc} = 0.7\omega_p$, $\omega_w = 0.1\omega_p$, and $\omega_m = 0.6\omega_p$; and the wave normal angle distributions are $[\phi_{lc}, \phi_{uc}] = [0, 20]°$ and $[\phi_m, \phi_w] = [10, 10]°$.

[e.g., *Summers et al.*, 2007b]. Then we determine the diffusion coefficients as a function of equatorial pitch angle α_{eq} and electron energy E_k in Figure 3. For radiation belt electrons of interest (>100 keV), only the first bounce-resonance harmonic $l = 1$ contributes to the pitch angle scattering at L = 4 and L = 5, as shown in Figure 2. At L = 3, no bounce resonance can be found for the first resonance harmonic ($l = 1$), while it is the $l = 2$ resonance that makes the major contribution to the bounce-resonant electron scattering. Our results demonstrate that electrons with α_{eq} ~90° are subject to very efficient bounce-resonant scattering (even exceeding $10^{-2}\,s^{-1}$), regardless of L shell or electron density. Figure 3 shows the weak dependence of bounce-resonant diffusion coefficients on electron density and their strong dependence on L shell for a given EMIC wave spectrum. Variation of electron density within an order of magnitude produces only slight changes of the bounce-resonant scattering rates, especially for electrons with α_{eq} >88°. In contrast, increase of L shell clearly broadens the α_{eq} coverage of efficient scattering rates ($>10^{-2}\,s^{-1}$). For instance, at L = 3, only α_{eq} >86° electrons can be scattered on time scales of ≤1 day due to bounce resonance with H^+ band EMIC waves. However, for L = 4 and 5, the corresponding efficient scattering region having a time scale of ≤1 day can extend to α_{eq} <70° and α_{eq} <60°, respectively. In addition, bounce resonance with H^+ band EMIC waves is more likely to occur for relativistic electrons at lower L shells, consistent with the results in Figure 2.

To make a quantitative comparison between bounce-resonance and cyclotron-resonance induced pitch angle scattering rates due to EMIC waves, we calculate the quasi-linear bounce-averaged pitch angle diffusion coefficients by cyclotron-resonant interactions with H^+ band EMIC waves, using the Full Diffusion Code [*Ni et al.*, 2008; *Shprits and Ni*, 2009]. This code has been extended by *Ni et al.* [2015] and *Cao et al.* [2016] to consider wave-induced particle diffusion in a cold, multi-ion (H^+, He^+, and O^+) plasma. Contributions from cyclotron resonance harmonics from $N = -5$ to $N = 5$ are included in our calculations. The results of bounce-averaged electron cyclotron-resonant pitch angle diffusion coefficients due to H^+ band EMIC waves are shown in Figure 4. As in Figure 3, we present the diffusion rates as a function of E_k and α_{eq} for

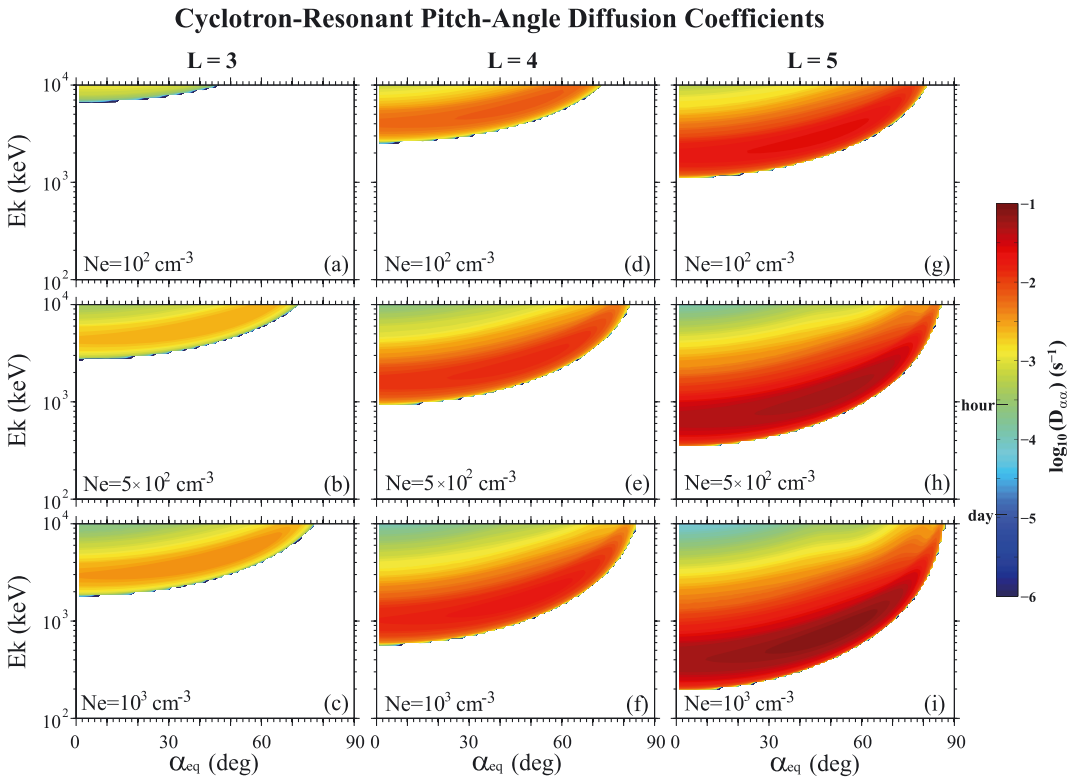

Figure 4. Same as Figure 3, except for cyclotron-resonant electron pitch angle diffusion rates due to H^+ band EMIC waves.

different L shells and electron number densities. Note that the wave amplitude, wave spectrum, normal angle distribution, ambient magnetic field, and cold ion composition ratios are identical to those used to produce the bounce-resonant diffusion rates in Figure 3. While bounce resonance with H^+ band EMIC waves results in efficient electron pitch angle scattering for α_{eq} ~75°–90°, cyclotron resonance dominates electron scattering at lower pitch angles extending all the way to the loss cone angle. A comparison between Figures 3 and 4 also shows a significant difference in variations of H^+ band EMIC wave-driven bounce- and cyclotron-resonant diffusion coefficients with ambient electron density. For cyclotron resonance, an increase of electron number density not only clearly affects the value profiles of diffusion coefficients but also significantly lowers the minimum resonant energy at any L shell. Similar to bounce-resonant scattering, cyclotron-resonant scattering tends to occur at lower electron energies as L shell increases. Increasing the L shell also results in stronger rates of pitch angle scattering, mainly due to the weaker intensity of the ambient magnetic field.

To further investigate the sensitivity of bounce-resonant pitch angle diffusion coefficients to EMIC wave normal angle distribution, spectral width, and peak frequency, we perform a careful analysis for various parameters. The computed results are illustrated as a function of E_k and α_{eq} in Figure 5 for L = 4. Specifically, Figures 5a–5c are reproduced from the second column of Figure 4 to show the effect of change in electron density. Figures 5d–5f show the effect of varying the wave normal angle distribution. Three normal angle distributions are specified: (1) $[\phi_{lc}, \phi_{uc}] = [0°, 20°]$ and $[\phi_m, \phi_w] = [10°, 10°]$, (2) $[\phi_{lc}, \phi_{uc}] = [15°, 45°]$ and $[\phi_m, \phi_w] = [30°, 15°]$, and (3) $[\phi_{lc}, \phi_{uc}] = [40°, 70°]$ and $[\phi_m, \phi_w] = [55°, 15°]$, representative of quasi-parallel propagation, intermediate-angle propagation, and highly oblique propagation, respectively. It is found that bounce-resonant electron scattering rates are strongly dependent on the obliquity of EMIC wave normal, peaking when the waves propagate at intermediate angles. A possible explanation is that an increase of EMIC wave obliquity enhances the parallel component of wavefield and subsequently causes stronger rates of bounce-resonant pitch angle scattering (see equations (2) and (3)). In Figures 5g–5i, we vary the spectral width $\omega_{uc} - \omega_{lc}$ (i.e., varying the lower and upper cutoff frequencies of H^+ band EMIC waves) by choosing $\omega_{uc} - \omega_{lc} = 0.15\omega_p$, $0.2\omega_p$, and $0.25\omega_p$. For a given peak wave frequency, an increase of the spectral width

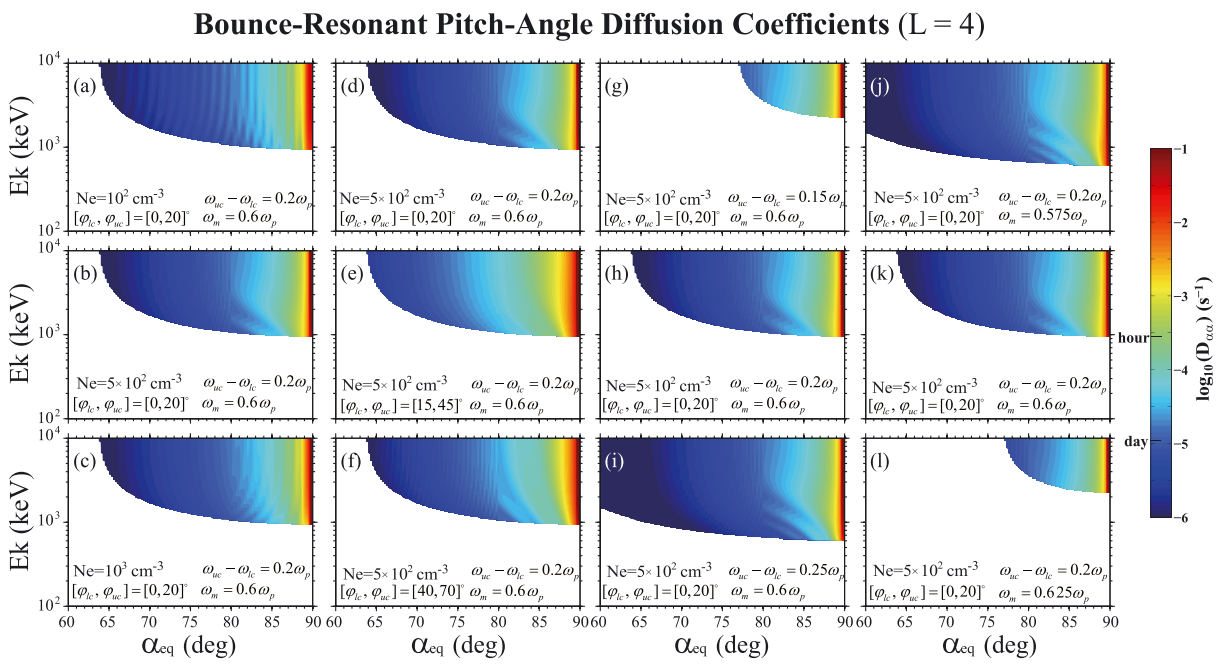

Figure 5. Bounce-resonant pitch angle diffusion coefficients due to the first-order resonance with 1 nT H^+ band EMIC waves at L = 4 for various parameter sets. Reproduced from the second column of Figure 4 to show the (a–c) effect of change in electron density; (d–f) varying wave normal angle distribution, i.e., [ϕ_{lc}, ϕ_{uc}] = [0, 20]° and [ϕ_m, ϕ_w] = [10, 10]°, [ϕ_{lc}, ϕ_{uc}] = [15, 45]° and [ϕ_m, ϕ_w] = [30, 15]°, and [ϕ_{lc}, ϕ_{uc}] = [40, 70]° and [ϕ_m, ϕ_w] = [55, 15]°; (g–i) varying the spectral width, i.e., $\omega_{uc} - \omega_{lc} = 0.15\omega_p$, $0.2\omega_p$, and $0.25\omega_p$; and (j–l) varying the peak wave frequency ω_m, i.e., $\omega_m = 0.575\omega_p$, $0.6\omega_p$, and $0.625\omega_p$.

results in much broader (E_k, α_{eq}) extent of bounce resonance and produces efficient bounce-resonant scattering at α_{eq} ~90° for lower energy electrons down to hundreds of keV. Finally, Figures 5j–5l show the effect of change in the peak wave frequency by choosing $\omega_m = 0.575\omega_p$, $0.6\omega_p$, and $0.625\omega_p$. Clearly, when the wave spectral width is fixed, an increase of peak wave frequency raises electron energies for bounce resonance with H^+ band EMIC waves.

Corresponding to Figure 5, EMIC wave-driven bounce-averaged cyclotron-resonant electron scattering rates are shown in Figure 6 for L = 4. In general, variations in wave spectral width and peak wave frequency can only introduce small differences in the cyclotron-resonant diffusion coefficients. H^+ band EMIC waves can cause cyclotron resonance with lower energy electrons when either the wave spectral width or the peak wave frequency increases. The ambient electron density and wave normal angle distribution are two critical factors that affect cyclotron-resonant scattering rates by H^+ band EMIC waves. Specifically, an increase of electron density enhances the cyclotron-resonant diffusion rates and shifts the peak to lower energies, while an increase in obliquity of EMIC waves tends to decrease the cyclotron-resonant diffusion rates.

Figure 7 shows the line plots of the bounce-resonant pitch angle diffusion coefficients due to H^+ band EMIC waves as a function of α_{eq} corresponding to different wave normal angle distributions, for L = 3.5, 4, and 4.5. In addition to the three wave normal angle distributions considered in Figure 5, we also adopt a nearly parallel propagation model with [ϕ_{lc}, ϕ_{uc}] = [0°, 10°] and [ϕ_m, ϕ_w] = [0°, 5°]. As illustrated in Figure 2, at L = 3.5, it is the second-order resonance $l = 2$ that contributes to the bounce-resonant scattering of radiation belt electrons. Owing to much lower resonant energies at L = 3.5, we show the results of diffusion coefficients for 0.2 and 0.4 MeV electrons. At L = 4 and 4.5, we show the pitch angle diffusion coefficients for 2 and 10 MeV electrons for the bounce-resonance order $l = 1$. Interestingly, the bounce-resonant diffusion coefficients tend to increase considerably with wave normal angle at small and intermediate values and then decrease gradually for highly oblique propagation. The L shell dependence of bounce-resonant scattering rate is also demonstrated. At L = 3.5, efficient pitch angle scattering on a time scale less than 1 day can only occur at $\alpha_{eq} > 84°$. As L increases to 4 and 4.5, pitch angle extents associated with efficient scattering on a time scale less than 1 day can extend to ~70° and ~60°, respectively.

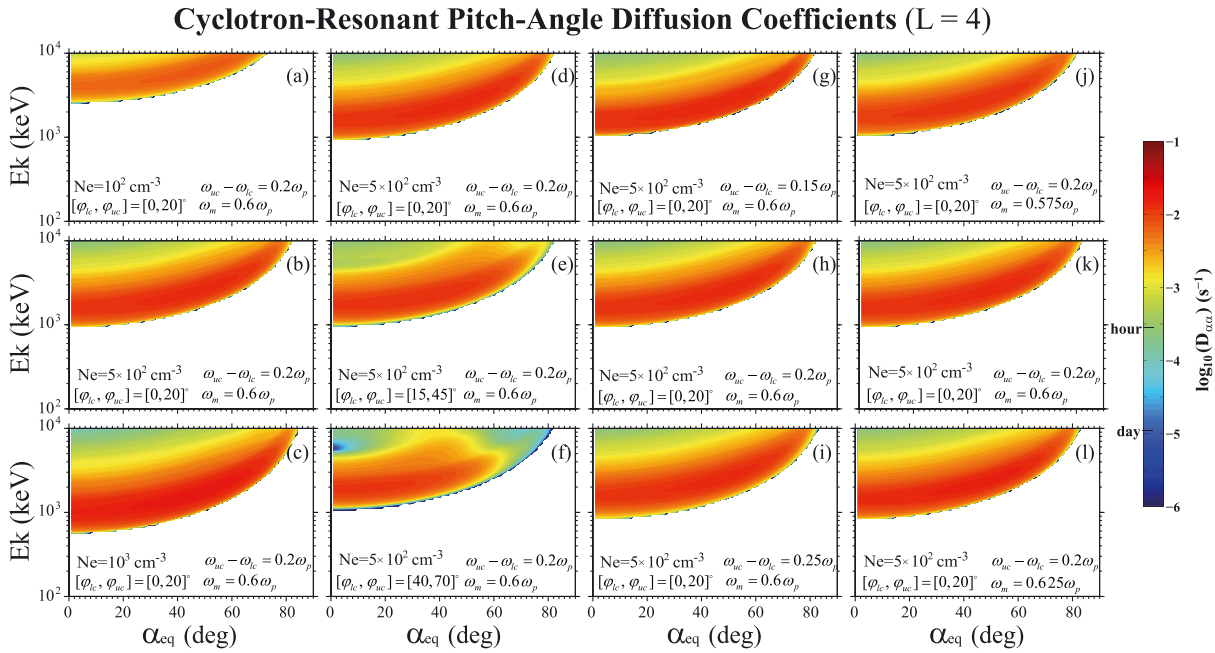

Figure 6. Same as Figure 5, except for cyclotron-resonant electron pitch angle diffusion rates due to H^+ band EMIC waves.

In Figure 8, we show the pitch angle diffusion coefficients of radiation belt electrons due to bounce and cyclotron resonance with H^+ band EMIC waves at L = 4 corresponding to two specific cases of wave latitudinal coverage: $\lambda_m = 40°$ (Figure 8, top) and $\lambda_m = 10°$ (Figure 8, bottom). Since the mirror latitudes of electrons with $\alpha_{eq} > 60°$ are not far from the magnetic equator [e.g., *Summers et al.*, 2007b, Figure 9], bounce-resonant diffusion coefficients for $\lambda_m = 40°$ are almost the same as those for $\lambda_m = 10°$. However, cyclotron-resonant diffusion coefficients vary significantly with a change in λ_m. Especially for electrons of energy ≥3 MeV, pitch angle scattering rates at smaller pitch angles decrease substantially when λ_m varies from 40° to 10°. This is because cyclotron-resonant regions for these ultra-relativistic electrons are mainly located at geomagnetic latitudes >10°.

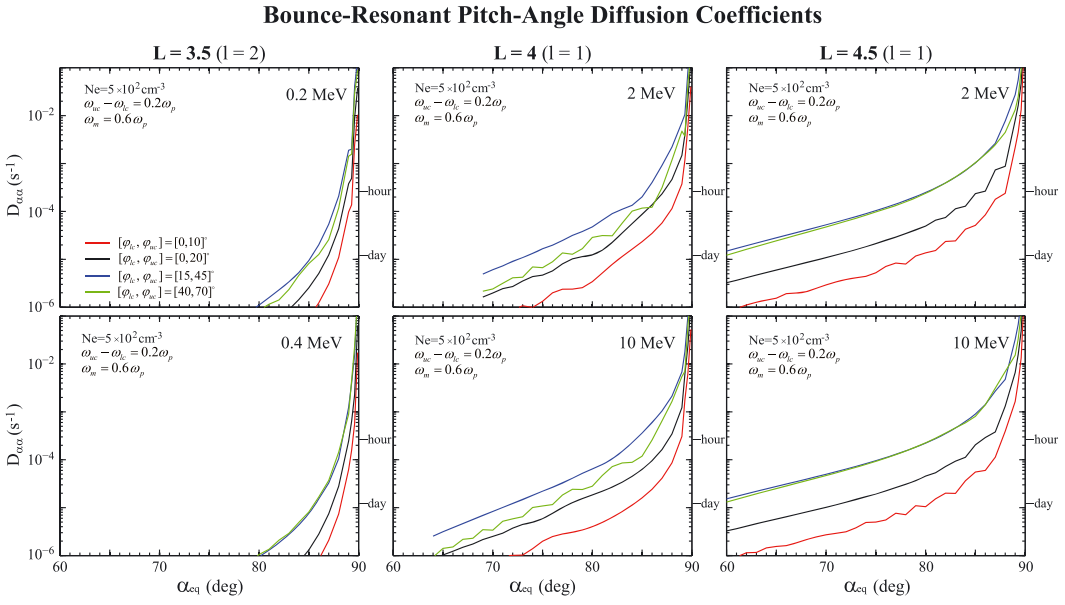

Figure 7. Line plots of bounce-resonant electron pitch angle diffusion coefficients as a function of equatorial pitch angle α_{eq} at L = 3.5, 4, and 4.5 for the indicated four wave normal angle distributions.

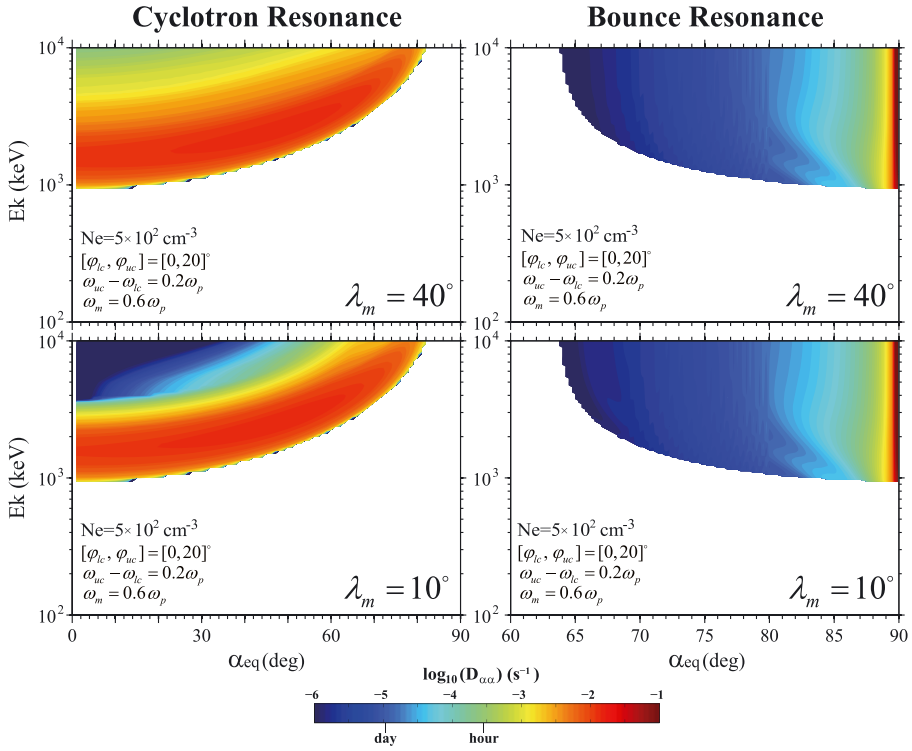

Figure 8. Comparisons between bounce- and cyclotron-resonant electron pitch angle diffusion coefficients by H^+ band EMIC waves at L = 4 for two specific cases of wave latitudinal coverage: (top) $\lambda_m = 40°$ and (bottom) $\lambda_m = 10°$.

4. Discussion and Conclusions

Our results clearly indicate that bounce-resonant and cyclotron-resonant pitch angle scatterings due to H^+ band EMIC waves occur at two distinct ranges of equatorial pitch angle. While bounce resonance predominantly occurs with radiation belt energetic electrons near 90°, cyclotron resonance primarily controls electron scattering at lower pitch angles. While H^+ band EMIC wave-driven bounce resonance alone cannot directly scatter near-equatorially mirroring electrons into the loss cone for diffusive loss, these electrons with decreased pitch angles can eventually undergo pitch angle scattering loss under the impact of cyclotron resonance, e.g., with H^+ band, He^+ band, and O^+ band EMIC waves, plasmaspheric hiss, or chorus waves. Therefore, it is suggested that bounce resonance due to EMIC waves, in combination with other wave-induced cyclotron resonance mechanisms, may contribute to the global coherency of electron fluxes at different pitch angles as well as storm time electron flux dropouts. This, however, requires future investigation.

As one of the most important distribution functions, the Gaussian distribution has been widely used to fit frequency spectra of magnetospheric waves, including chorus, hiss, magnetosonic, and EMIC waves [e.g., *Li et al.*, 2007; *Horne et al.*, 2007; *Summers et al.*, 2007a, 2007b]. The Gaussian distribution can basically capture the spectral properties of waves and can also be easily incorporated into the mathematical calculations. Even though an arbitrary wave spectrum could be adopted for our calculations, for simplicity and with little loss of generality, in the present study, we have assumed that the H+ band wave frequency distribution is Gaussian.

It should be noted that, once thermal effects introduced by warm or hot ions are strong enough, the dispersion relation of EMIC waves will be significantly modified and the cold plasma approximation will no longer be valid [e.g., *Isenberg*, 1984; *Brinca and Tsurutani*, 1987; *Lui et al.*, 1987]. In contrast to the cyclotron resonance condition, the bounce resonance condition (equation (9)) is only dependent on wave frequency and is independent on wave number. This indicates that, for a given wave spectrum, inclusion of the warm plasma effects only influences the diffusion coefficients, which are strongly dependent on wave number, but does not affect the energy range of resonant electrons. Although the cold plasma

approximation has been used in this study for simplicity, it will be worthwhile in the future to take into account warm plasma effects in order to evaluate more precisely the bounce-resonant interactions of electrons with EMIC waves. In the present study, we follow previous studies and choose a representative set of ion concentration ratios (H^+: He^+: O^+ = 0.85: 0.10: 0.05). However, O^+ abundances can be highly variable and minor ion abundances play a role in the dispersion relation and the calculation of the diffusion coefficients. Some previous studies have used linear kinetic theory [e.g., *Mace et al*., 2011; *Henning and Mace*, 2014; *Wang et al*., 2016] or hybrid simulations [e.g., *Denton and Hu*, 2010; *Denton et al*., 2014] to show that high He^+ abundance or high O^+ ion abundance strongly suppresses the growth of H^+ band EMIC waves. Since this study focuses on the role of H^+ band EMIC waves in driving the bounce resonance with radiation belt electrons, we have therefore adopted the above set of ion concentration ratios for our numerical calculations. We note that it will be of future interest to investigate the sensitivity of bounce-resonant interactions between H^+ band EMIC waves and radiation belt electrons to the variation in ion concentration ratios.

As suggested by *Shprits* [2016], if the time scale associated with wave-induced pitch angle scattering is only a few times longer than the electron bounce period or even less than one bounce period, then the method used in the calculations of bounce-resonant diffusion coefficients becomes no longer valid. And we note that, as we have shown in Figure 7, if the equatorial pitch angle of electrons is very close to 90°, say, 89° to 90°, then the time scale associated with pitch angle scattering could be shorter than 10 s, which is comparable to the electron bounce period. Therefore, the diffusion coefficients may not precisely represent the radiation belt energetic electron dynamics when interacting with EMIC waves but simply serve as an indication of very strong scattering. It has been recognized that nonlinear effects [e.g., *Chen et al*., 2015; *Maldonado et al*., 2016] can be involved in the bounce-resonant interactions between equatorially mirroring electrons and magnetosonic waves. Similarly, nonlinear effects introduced by intense EMIC emissions should also be taken into account in evaluations of bounce-resonant electron scattering. Specifically, *Maldonado et al*. [2016] considered bounce-resonant scattering as "advection" instead of "diffusion" since strong scattering due to nonlinear wave-particle interactions is systematic or advective. The calculations of the diffusion coefficients in the present study are based on the quasi-linear diffusion regime, in which electromagnetic waves cause a random walk of a particle's second invariant and the corresponding scattering is stochastic [*Roberts and Schulz*, 1968]. In fact, nonlinear theory should be taken into account to evaluate more precisely the strong pitch angle scattering of electrons with an equatorial pitch angle very close to 90°. It will then be more appropriate to use "advection" to describe the pitch angle scattering process. Such an analysis, however, is outside the scope of the present study.

In this study we have performed a comprehensive analysis of bounce-resonant interactions between H^+ band EMIC waves and radiation belt energetic electrons by investigating in detail the sensitivity of bounce-resonant scattering rates to L shell, ambient electron density, wave normal angle distribution, wave spectral properties, and wave latitudinal extent. Quantitative comparisons have also been performed between bounce-resonant and cyclotron-resonant diffusion coefficients due to scattering by H^+ band EMIC waves. Our major conclusions are summarized as follows:

1. H^+ band EMIC waves can bounce-resonate with near-equatorially mirroring electrons over a wide range of energies and L shells. Resonant regions in (E_k, L shell) space where bounce-resonant interactions can take place are predominantly determined by the wave spectrum and the resonance order.
2. For $>$100 keV radiation belt electrons, bounce resonance with H^+ band EMIC waves plays as an efficient mechanism to transport them from near 90° pitch angles to lower pitch angles on time scales of hours or less. Resultant bounce-resonant scattering rates tend to show a weak dependence on ambient electron density and wave latitudinal extent but a strong dependence on L shell, wave normal angle distribution, and wave frequency spectrum. Cyclotron-resonant scattering rates due to H^+ band EMIC waves are very sensitive to ambient electron density, wave latitudinal extent, and wave normal angle distribution.
3. Bounce resonance and cyclotron resonance by H^+ band EMIC waves, in combination, have the potential to transport near-equatorially mirroring electrons to lower pitch angles and then diffuse them into the loss cone for precipitation loss. This may explain the global coherency of electron fluxes at different pitch angles and contribute to storm time electron flux dropouts.

Acknowledgments
This work was supported by the NSFC grants 41674163, 41474141, and 41204120. No observational data were used in the present study. D.S. holds the position of overseas prominent professor at Wuhan University and wishes to thank the Department of Space Physics for the excellent hospitality during his visits. D.S. also acknowledges support from a discovery grant of the Natural Sciences and Engineering Research Council of Canada. X.T. would like to acknowledge the support by NSFC grant 41474142. J.B. would like to acknowledge grants NNX13AI61G and NNX14AN85G.

References

Albert, J. M. (2003), Evaluation of quasi-linear diffusion coefficients for EMIC waves in a multispecies plasma, *J. Geophys. Res.*, *108*(A6), 1249, doi:10.1029/2002JA009792.

Albert, J. M. (2007), Simple approximations of quasi-linear diffusion coefficients, *J. Geophys. Res.*, *112*, A12202, doi:10.1029/2007JA012551.

Brinca, A. L., and B. T. Tsurutani (1987), Unusual characteristics of electromagnetic waves excited by newly born ions with large perpendicular energies, *Astron. Astrophys.*, *187*, 311–319.

Cao, X., et al. (2016), Resonant scattering of central plasma sheet protons by multiband EMIC waves and resultant proton loss timescales, *J. Geophys. Res. Space Physics*, *121*, 1219–1232, doi:10.1002/2015JA021933.

Chen, L., A. Maldonado, J. Bortnik, R. M. Thorne, J. Li, L. Dai, and X. Zhan (2015), Nonlinear bounce resonances between magnetosonic waves and equatorially mirroring electrons, *J. Geophys. Res. Space Physics*, *120*, 6514–6527, doi:10.1002/2015JA021174.

Denton, R. E., and Y. Hu (2010), Two-dimensional hybrid simulation of the growth, effects, and distribution of magnetospheric electromagnetic ion cyclotron waves, Abstract SM21D-03 presented at 2010 Fall Meeting, AGU, San Francisco, Calif., 13-17 Dec.

Denton, R. E., V. K. Jordanova, and B. J. Fraser (2014), Effect of spatial density variation and O^+ concentration on the growth and evolution of electromagnetic ion cyclotron waves, *J. Geophys. Res. Space Physics*, *119*, 8372–8395, doi:10.1002/2014JA020384.

Elkington, S. R., M. K. Hudson, and A. A. Chan (2003), Resonant acceleration and diffusion of outer zone electrons in an asymmetric geomagnetic field, *J. Geophys. Res.*, *108*(A3), 1116, doi:10.1029/2001JA009202.

Glauert, S. A., and R. B. Horne (2005), Calculation of pitch angle and energy diffusion coefficients with the PADIE code, *J. Geophys. Res.*, *110*, A04206, doi:10.1029/2004JA010851.

He, F., X. Cao, B. Ni, Z. Xiang, C. Zhou, X. Gu, Z. Zhao, R. Shi, and Q. Wang (2016), Combined scattering loss of radiation belt relativistic electrons by simultaneous three-band EMIC waves: A case study, *J. Geophys. Res. Space Physics*, *121*, 4446–4451, doi:10.1002/2016JA022483.

Henning, F. D., and R. L. Mace (2014), Effects of ion abundances on electromagnetic ion cyclotron wave growth rate in the vicinity of the plasmapause, *Phys. Plasmas*, *21*, 042905, doi:10.1063/1.4873375.

Horne, R. B., and R. M. Thorne (1998), Potential waves for relativistic electron scattering and stochastic acceleration during magnetic storms, *Geophys. Res. Lett.*, *25*, 3011–3014, doi:10.1029/98GL01002.

Horne, R. B., R. M. Thorne, S. A. Glauert, N. P. Meredith, D. Pokhotelov, and O. Santolík (2007), Electron acceleration in the Van Allen radiation belts by fast magnetosonic waves, *Geophys. Res. Lett.*, *34*, L17107, doi:10.1029/2007GL030267.

Hudson, M. K., D. N. Baker, J. Goldstein, B. T. Kress, J. Paral, F. R. Toffoletto, and M. Wiltberger (2014), Simulated magnetopause losses and Van Allen Probe flux dropouts, *Geophys. Res. Lett.*, *41*, 1113–1118, doi:10.1002/2014GL059222.

Isenberg, P. A. (1984), The ion cyclotron dispersion relation in a proton-alpha solar wind, *J. Geophys. Res.*, *89*, 2133–2141, doi:10.1029/JA089iA04p02133.

Lenchek, A., S. Singer, and R. Wentworth (1961), Geomagnetically trapped electrons from cosmic ray albedo neutrons, *J. Geophys. Res.*, *66*, 4027–4046, doi:10.1029/JZ066i012p04027.

Li, W., Y. Y. Shprits, and R. M. Thorne (2007), Dynamic evolution of energetic outer zone electrons due to wave-particle interactions during storms, *J. Geophys. Res.*, *112*, A10220, doi:10.1029/2007JA012368.

Li, X., X. Tao, Q. Lu, and L. Dai (2015), Bounce resonance diffusion coefficients for spatially confined waves, *Geophys. Res. Lett.*, *42*, 9591–9599, doi:10.1002/2015GL066324.

Lui, A. T. Y., R. W. McEntire, and S. M. Krimigis (1987), Evolution of the ring current during two geomagnetic storms, *J. Geophys. Res.*, *92*, 7459–7470, doi:10.1029/JA092iA07p07459.

Lyons, L. R. (1974), Pitch angle and energy diffusion coefficients from resonant interactions with ion-cyclotron and whistler waves, *J. Plasma Phys.*, *12*, 417–432, doi:10.1017/S002237780002537X.

Mace, R. L., R. D. Sydora, and I. Silin (2011), Effects of superthermal ring current ion tails on the electromagnetic ion cyclotron instability in multi-ion magnetospheric plasmas, *J. Geophys. Res.*, *116*, A05206, doi:10.1029/2010JA016393.

Maldonado, A. A., L. Chen, S. G. Claudepierre, J. Bortnik, R. M. Thorne, and H. Spence (2016), Electron butterfly distribution modulation by magnetosonic waves, *Geophys. Res. Lett.*, *43*, 3051–3059, doi:10.1002/2016GL068161.

Meredith, N. P., R. M. Thorne, R. B. Horne, D. Summers, B. J. Fraser, and R. R. Anderson (2003), Statistical analysis of relativistic electron energies for cyclotron resonance with EMIC waves observed on CRRES, *J. Geophys. Res.*, *108*(A6), 1250, doi:10.1029/2002JA009700.

Meredith, N. P., R. B. Horne, T. Kersten, B. J. Fraser, and R. S. Grew (2014), Global morphology and spectral properties of EMIC waves derived from CRRES observations, *J. Geophys. Res. Space Physics*, *119*, 5328–5342, doi:10.1002/2014JA020064.

Min, K., J. Lee, K. Keika, and W. Li (2012), Global distribution of EMIC waves derived from THEMIS observations, *J. Geophys. Res.*, *117*, A05219, doi:10.1029/2012JA017515.

Ni, B., R. M. Thorne, Y. Y. Shprits, and J. Bortnik (2008), Resonant scattering of plasma sheet electrons by whistler-mode chorus: Contribution to diffuse auroral precipitation, *Geophys. Res. Lett.*, *35*, L11106, doi:10.1029/2008GL034032.

Ni, B., et al. (2015), Resonant scattering of outer zone relativistic electrons by multiband EMIC waves and resultant electron loss time scales, *J. Geophys. Res. Space Physics*, *120*, 7357–7373, doi:10.1002/2015JA021466.

Roberts, C., and M. Schulz (1968), Bounce resonant scattering of particles trapped in the Earth's magnetic field, *J. Geophys. Res.*, *73*, 7361–7376, doi:10.1029/JA073i023p07361.

Roederer, J. G. (1970), *Dynamics of Geomagnetically Trapped Radiation*, Springer, New York, doi:10.1007/978-3-642-49300-3.

Schulz, M., and L. J. Lanzerotti (1974), *Particle Diffusion in the Radiation Belts, Physics and Chemistry in Space*, vol. 7, pp. 215, Springer, New York.

Shprits, Y. Y. (2009), Potential waves for pitch angle scattering of near-equatorially mirroring energetic electrons due to the violation of the second adiabatic invariant, *Geophys. Res. Lett.*, *36*, L12106, doi:10.1029/2009GL038322.

Shprits, Y. Y. (2016), Estimation of bounce resonant scattering by fast magnetosonic waves, *Geophys. Res. Lett.*, *43*, 998–1006, doi:10.1002/2015GL066796.

Shprits, Y. Y., and B. Ni (2009), Dependence of the quasi-linear scattering rates on the wave normal distribution of chorus waves, *J. Geophys. Res.*, *114*, A11205, doi:10.1029/2009JA014223.

Shprits, Y. Y., D. A. Subbotin, N. P. Meredith, and S. R. Elkington (2008a), Review of modeling of losses and sources of relativistic electrons in the outer radiation belts: II. Local acceleration and loss, *J. Atmos. Sol. Terr. Phys.*, *70*(14), 1694–1713, doi:10.1016/j.jastp.2008.06.014.

Shprits, Y. Y., S. R. Elkington, N. P. Meredith, and D. A. Subbotin (2008b), Review of modeling of losses and sources of relativistic electrons in the outer radiation belts: I. Radial transport, *J. Atmos. Sol. Terr. Phys.*, *70*(14), 1679–1693, doi:10.1016/j.jastp.2008.06.008.

Stix, T. H. (1962), *The Theory of Plasma Waves*, McGraw-Hill, New York.

Summers, D., and R. M. Thorne (2003), Relativistic electron pitch angle scattering by electromagnetic ion cyclotron waves during geomagnetic storms, *J. Geophys. Res.*, *108*(A4), 1143, doi:10.1029/2002JA009489.

Summers, D., R. M. Thorne, and F. Xiao (1998), Relativistic theory of wave-particle resonant diffusion with application to electron acceleration in the magnetosphere, *J. Geophys. Res.*, *103*, 20,487–20,500, doi:10.1029/98JA01740.

Summers, D., B. N. Ni, and N. P. Meredith (2007a), Timescales for radiation belt electron acceleration and loss due to resonant wave-particle interactions: 2. Evaluation for VLF chorus, ELF hiss, and electromagnetic ion cyclotron waves, *J. Geophys. Res.*, *112* A04207, doi:10.1029/2006JA011993.

Summers, D., B. Ni, and N. P. Meredith (2007b), Timescales for radiation belt electron acceleration and loss due to resonant wave-particle interactions: 1. Theory, *J. Geophys. Res.*, *112*, A04206, doi:10.1029/2006JA011801.

Tao, X., and X. Li (2016), Theoretical bounce resonance diffusion coefficient for waves generated near the equatorial plane, *Geophys. Res. Lett.*, *43*, 7389–7397, doi:10.1002/2016GL070139.

Thorne, R. M. (2010), Radiation belt dynamics: The importance of wave-particle interactions, *Geophys. Res. Lett.*, *37*, L22107, doi:10.1029/2010GL044990.

Wang, Q., X. Cao, X. Gu, B. Ni, C. Zhou, R. Shi, and Z. Zhao (2016), A parametric study of the linear growth of magnetospheric EMIC waves in a hot plasma, *Phys. Plasmas*, *23*, 062903, doi:10.1063/1.4953565.